Electrochimica Acta 456 (2023) 142465

Contents lists available at ScienceDirect

Electrochimica Acta

journal homepage: www.journals.elsevier.com/electrochimica-acta

Guanine adsorption on gold electrodes studied by in situ surface-enhanced infrared reflection absorption spectroscopy

Julia Alvarez-Malmagro *, Manuela Rueda, Francisco Prieto-Dapena *

Departamento de Química Física, Universidad de Sevilla, C/ Profesor García González n 2, 41012 Seville, Spain

ARTICLE INFO

Keywords:
guaninie adsorption
gold electrodes
tautomerism
Attenuated Total Reflection Surface-Enhanced Infrared Absorption Spectroscopy

ABSTRACT

The adsorption of guanine on single-crystal and thin-film gold electrodes has been explored by combination of cyclic voltammetry and ATR-SEIRA 'in situ' spectroscopy at two pD values (8 and 11.6) employing D_2O as a solvent. The experimental conditions are selected to study the adsorption / desorption of the two forms of guanine involved in the second acid-base equilibria and its tautomeric forms.

The ATR-SEIRA spectra of adsorbed guanine were compared to the absorption FT-IR spectra in solution and interpreted in light of DFT calculations of the different acid-base and tautomeric forms with different solvation states of the CO group. Furthermore, the preponderance of each tautomeric form and the possible changes in orientation with the electric field have been determined by analyzing the two-dimensional correlation spectrum (2D COS) as well as the influence of the potential on the integrated intensities of the spectral signals in the 1800–1400 cm^{-1} region. It has been found that at pD 8 the adsorbed keto-amino tautomer of neutral guanine predominates in solution and in adsorbed state, and adsorbed guanine slightly rotate its molecular plane with the potential. At pD 11.6 the keto-amino tautomer of anionic guanine is the unique form detectable in the solution, while in adsorbed state the keto-imino tautomeric form is also present with its preponderance increasing with the electrode potential.

1. Introduction

Guanine (G), a planar molecule formed by fusion of a pyrimidine and an imidazole ring, is involved in two acid-base equilibria in aqueous solutions (Scheme 1). The first, pKa1 = 4.2, is related to the protonation of the imidazole nitrogen N7 while the second, pKa2 = 9.5, accounts for the loss of proton in the pyrimidine nitrogen N1 [1,2].

Guanine is one of the two purine DNA bases found in nucleic acids that are present in the genetic material of all living organisms and plays an important role in genetic expression and replication. These processes are related to guanine base pairing in DNA with its complementary base, cytosine, Watson and Crick interactions through three H-bonds [3] (scheme 2). It has been postulated that the presence of "rare" tautomeric forms in the genetic material may be responsible for genetic errors, via base mispairing formation during polymerase-mediated DNA replication, resulting in genetic mutations[2,4]. However, only the ratio of unfavorable tautomer in solution between 10^{-4} and 10^{-5} do not allow to explain the high number of mutations in the DNA[4]. Sowers et al. [5] have proposed that hydrogen-bonding interactions and base pair formation could be perturbed by base ionization and predicted that the ionized forms might exist several orders of magnitude more frequently than the rare tautomeric forms [5] and in consequence are also responsible of DNA mutations [6]. So that the study of the behavior of guanine, its structural and conformational preferences as well as its physicochemical properties is vital to understand the biochemical processes in which it is involved.

Several theoretical studies have been leading to the tautomerism of guanine. However, there is still some controversy regarding which form is the favored guanine specie. Chandra et al. [7] demonstrated that solvation effects are known to be vital in the interaction between guanine and cytosine because specific solvation of the N3 and N7 sites of guanine can modify the intrinsic acidities or basicities of the other site. More recently, Jang et al. [2] shown that tautomeric configuration of guanine can be drastically different depending on the environment. They found that neutral guanine is in the aqueous phase as keto-amino tautomer, This keto-amino forms are also the main species present in the gas phase, but with the presence of some enol-amino tautomer. On the other hand, Carvalho et al. [6] combined vibrational spectroscopy

* Corresponding authors.
E-mail addresses: jalvarez21@us.es (J. Alvarez-Malmagro), dapena@us.es (F. Prieto-Dapena).

https://doi.org/10.1016/j.electacta.2023.142465
Received 21 December 2022; Received in revised form 6 March 2023; Accepted 21 April 2023
Available online 22 April 2023

techniques coupled with quantum mechanical methods at the DFT level and found that the keto-amino tautomer with H in position 7 was the preponderant form at the condensed state as well as for the isolated molecule, contrary to aqueous solutions and hydrated polycrystalline guanine, where the canonical keto-amino tautomer with H in position 9 is found to be the most favoured species. These studies are critical in the development of the rare tautomer hypothesis of spontaneous mutagenesis which consider that mutations arise through the formation of unstable tautomers[8]. In deep, it is known that some diseases or pathogenesis such as cystic fibrosis, sickle cell anemia, and Alzheimer's disease [9,10] are related to these kind of mutations in the DNA.

The study of the tautomerism of DNA bases adsorbed on solid electrodes is an attractive task due to the electrostatic similarities between solid electrode/electrolyte interfaces and biological interfaces. To our knowledge, there have only been a few works considering adsorption of guanine on different solid-material electrodes. On graphite solid electrodes, STM and AFM at atomic resolution measurements have concluded that guanine is adsorbed parallel to the electrode surface in a two-dimensional ordered structure packing into a rectangular lattice [11]. On HOPG electrodes, guanine condenses in a monolayer film with a flat orientation under potential control[12]. On gold electrodes, adsorption of guanine takes place in different adsorbed states that depend on the applied potential[13]. With specular reflectivity measurements Takamura et al. have found that guanine is adsorbed in a different way at negatively or positively charged electrodes, either in orientation or because of dimerization[14]. Further STM and AFM measurement combined with cyclic voltammetry [13] allowed to visualize disorder polymeric aggregated in which guanine molecules are stacked on the gold surface.

In this work, the adsorption of guanine on gold thin film electrodes is studied by ATR-SEIRA in situ spectroscopy, in the Kretschmann configuration, in neutral and basic media to determine the adsorption behavior of the different ionized and/or tautomeric forms of guanine. Electrochemical measurements have been carried out at two pH values at which either the neutral or anionic form exist in solution. The previous studies developed by Ferapontova in an acidic medium show oxidation at such low potentials that there is no range accessible of potentials at which to study the double layer[15]. For interpretation, the spectroscopic results in deuterated media have been compared with the DFT calculated spectra of different ionized or tautomeric forms of guanine. This allowed us to determine the preponderance of each form of guanine as a function of pH and of the applied potential. Furthermore, the influence of the electric field on the molecular plane orientation of the adsorbed forms has been determined by analyzing the integrated intensities of the signals in the 1800 – 1400 cm^{-1} region.

2. Materials and methods

2.1. Reagents, electrodes and solutions

The chemicals were purchased from Sigma-Aldrich and used without any further purification.

Supporting electrolyte solutions (0.1 M NaF at pH 8 and 0.1 M NaF + NaOH at pH 11.6) were prepared either in deuterium oxide (Sigma Aldrich 99.99%) or ultrapure water purified with a Millipore Milli-Q systems. Working solutions of guanine of the desired concentration were obtained by dosing in the electrochemical or spectroelectrochemical cell the required amount of stock solution of the DNA base prepared in the same supporting electrolyte. Stock solutions of guanine were prepared in the maximun concentration allow to dissolve guanine; 0.025 mM at pH 8 and 1 mM at 11.6. A glass membrane combined electrode from Hamilton was employed to measure the pH of all solutions. In D_2O solutions, pH values were corrected according to $pD = pH + 0.4$ [16]

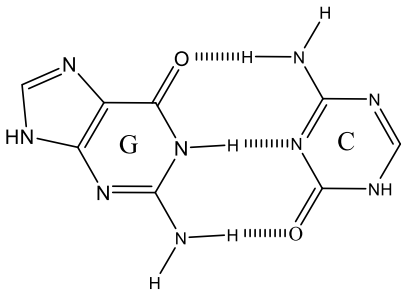

Scheme 2. Watson and Crick (WC) interaction between guanine (G) and cytosine (C).

2.2. Electrochemical measurements

Electrochemical measurements were recorded with an Ecochemie Autolab PGstat 30 instrument and with an IviumStat from Ivium Technologies. Cyclic voltammetry was conducted in a three-electrode glass cell at 50 mV s^{-1}. A freshly flame-annealed Au (111) electrode prepared according to the Clavilier method [17] was used as working electrode and contacted with the working solution by the meniscus method. A flame-annealed gold wire and a saturated mercury/mercurous sulfate electrode, connected to the cell by an intercalated salt-bridge filled with the same supporting electrolyte, were used as a counter and reference electrodes, respectively. All potentials are given respect to a saturated calomel reference electrode, SCE ($E_{SCE} = E_{mercury/mercurous\ sulfate} + 0.4$ V). Before any measurements, the electrochemical cell was deaerated by bubbling high purity argon, for 30 min. After that, a blanket of the inert gas was kept over the working solution during the measurements.

The capacitance vs potential plots were obtained assuming a series RC circuit from the EIS measurement performed with an Autolab PGSTAT 30, equipped with a FRA module. The frequency and amplitude of the AC perturbation were 25 Hz and 10 mV, respectively. The d.c. potential was changed in steps of 20 mV and kept constant during the impedance measurement.

2.3. Fourier transform infrared (FT-IR) spectroscopy measurements

2.3.1. ATR-SEIRAS measurements

In situ spectroelectrochemical ATR-SEIRA spectra were obtained with a resolution of 4 cm^{-1} using a NICOLET 6700 spectrophotometer endowed with an MCT-A detector and a VeeMaxTM-II accessory from PIKE Technologies for reflectance measurements. A CHI 1100 potentiostat from CH Instruments was used for the electrochemical control of the spectrochemical cell. 100 reflectance spectra at different potentials have been collected with p-polarized light (polarized in the incidence

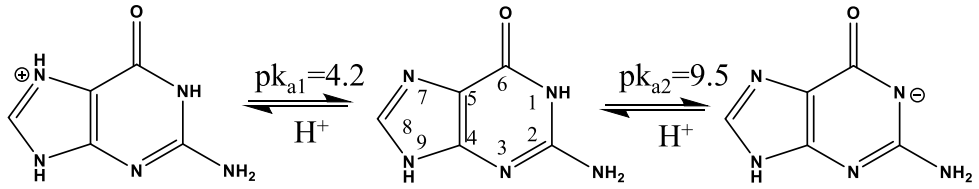

Scheme 1. Acid-base equilibrium of guanine.

plane), selected with ZnSe motorized polarized and then averaged. The final absorbance spectra are represented as logarithmic (R_0 / R) where R_0 and R are the reflectance spectrum of the reference and sample, respectively in the same working conditions. A setup based on the Kretschmann configuration for internal reflection was used. A silicon prism beveled at 60° was used as an IR window. The working electrode consists of a gold film of 20–25 nm thickness, deposited by sputtering (at ca. 0.01 nm s^{-1} with a Leica EM SCD500 metallizer, equipped with a quartz crystal microbalance) was placed on one of the faces of the prism. A gold foil and saturated mercury/mercurous sulfate electrodes were employed as a counter and reference electrodes, respectively.

Previously to any set of spectroscopy measurements, the cell was purged by bubbling high purity nitrogen. In all experiments, the background spectra (R_0) at different potentials were collected in the absence of guanine. The electrode potential was changed at 10 mV s^{-1}, between measurement potentials, and it was kept constant during the spectra acquisition. Then, the exact volume of the stock solution of guanine was added to the electrochemical cell to obtain the desired concentration of DNA bases in the cell. Finally, the reflectance spectra of the sample (R) were collected following the same procedure than in the absence of guanine.

The value of the integrated intensity (A) of an ATR-SEIRAS band is proportional to both, the surface concentration of the adsorbed species (Γ) and to the squared cosine of the angle between the vibrational transition dipole and the normal direction to the adsorbing surface, (θ), as it is shown in Eq. (1). [18]

$$A \propto \Gamma \cos^2(\theta) \quad (1)$$

2.3.2. Transmission IR spectra measurements

Absorption spectra in solution were obtained in two ways: transmission IR spectra of 10 mM guanosine-5-diphosphate (Sigma-Aldrich) in D_2O at pD 8 were measured as previously described [19] using a homemade Teflon cell equipped with two circular CaF_2 windows separated by a 50 μm Teflon spacer. For 9 mM guanine in D_2O at pD 11.6, the same ATR cell used for spectroelectrochemical measurements was employed, but with a 45° ZnSe prismatic optical window to achieve a better correction of the solvent absorption bands. In both approaches a total of 1000 scans were collected using a resolution of 4 cm^{-1}.

2.4. DFT details

The geometry and vibrations properties of guanine in gas phase have been modeled employing a hybrid functional PBE as implemented in the Gaussian 09 software [20] and a basis sets 6–311+*G*(d,p)[21–23]. The calculations have also been performed including two or three water molecules in order to consider the solvation of carbonyl group. The theoretical vibrational frequencies have been corrected by optimized scaling factors for the functional and basis sets used[24].

For calculations with adsorbed guanine on Au(111) surfaces, a layer of 84 atoms of gold with a fixed geometry was used. The functional PBE and the 6–311 + G(d) basis sets for C, N, O, and H atoms and the semi-empirical PM6 method for Au atoms were used.

3. Results and discussion

3.1. Cyclic voltammetry

Fig. 1 shows the stationary cyclic voltammograms obtained with flame-annealed Au (111) electrodes immersed in solutions containing guanine at pH 8 and 11.6. At these values, it is possible to observe the capacitative region in a wide potential range, contrary to observed in acid media[15]. The voltammograms in the double layer potential region, as well as the capacitance curve at pD 11.6 (Fig. S1 in SI) substantiate that an adsorbed layer of guanine is formed from the more negative potential values. These results also reveal different adsorption

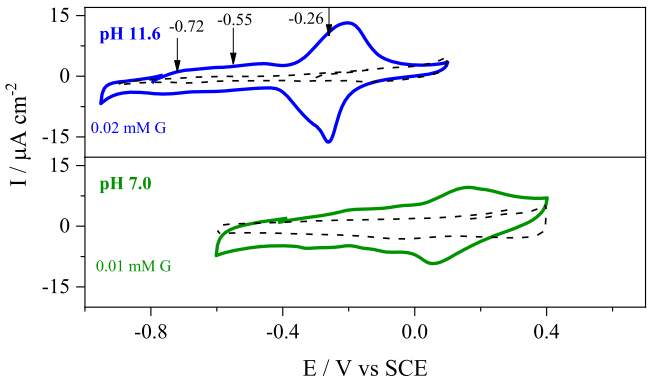

Fig. 1. Cyclic voltammograms obtained with Au(111) electrodes at 50 mV s^{-1} for solutions containing guanine (G) at the indicated concentrations and pH values. The black dashed lines correspond to the voltagramograms of the supporting electrolytes at 50 mV s^{-1}. Arrows in upper panel mark the positon of the capacitance peaks in figure S1.

regions that are not separated by phase transition peaks. Tao et al.[13]. have previously studied guanine adsorption on Au(111) by scanning tunneling microscopy (STM) and atomic force microscopy (AFM) observing that guanine adsorbed spontaneously on the gold electrode forming polymeric aggregates, which is in good agreement with our voltammetry results. Fig. 1 also reveals the influence of electrolyte pH on adsorption / desorption processes. Thus, as the solution pH increases the adsorption /desorption peaks of guanine shift toward lower potential values. This potential shift is similar to that observed for the adsorption of anionic or neutral adenine on gold electrodes at basic or neutral pH, respectively[25].

3.2. FT-IR spectra of guanine in solution

At pD 8, to overcome the low solubility of neutral guanine[26], we have employed guanosine 5′-diphosphate (G 5DP) which has the same structure of guanine although the hydrogen in N9 is substituted by a sugar ring. Therefore, it can be expected that at wavenumbers in the 1400–1800 cm^{-1} range the spectra of G-5DP and guanine are coincident. The experimental spectra of G 5DP in solution at pD 8 and guanine at pD 11.6 are given in Fig. 2.

In Fig. 2a, three strong bands at 1662, 1579 and 1565 cm^{-1} and a weak band at 1539 cm^{-1} are observed for G-5DP in solution. Scheme 3a contains the three main tautomeric forms of neutral guanine. The presence of a strong band at 1662 cm^{-1} suggests the existence of carbonyl group responsible for this absorption signal. Therefore, the enol tautomer of neutral guanine could be discarded. In order to decide

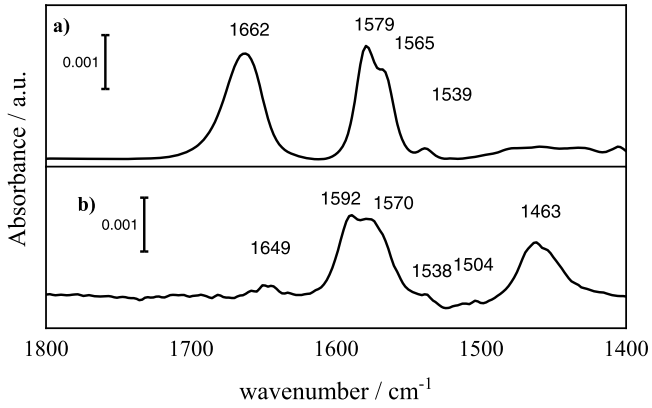

Fig. 2. a). FT-IR spectra of guanosine 5′-diphosphate in D_2O solution at pD 8, b).) FT-IR spectra of anionic guanine in D_2O solution at pD 11.6.

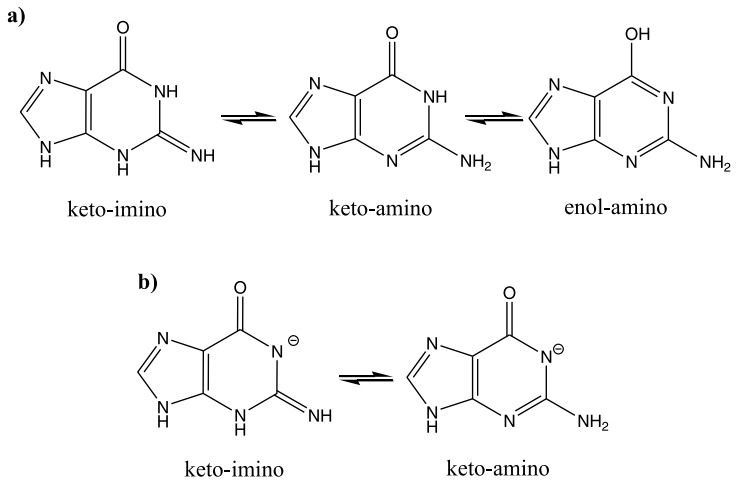

Scheme 3. Main tautomeric forms of a) neutral guanine and b) anionic guanine.

the preponderant tautomer in solution (keto-amino or keto-imino) and to obtain the assignations and the directions of the transition dipoles of the corresponding vibrations, DFT simulations of the theoretical spectra for guanine in D_2O have been obtained, with a previous geometrical optimization. In Fig. S2 of SI file, the experimental spectrum of G-5DP is compared to the theoretical vibrational spectra obtained from DFT calculations, with a previous geometrical optimization, over the keto-amino and keto-imino tautomers. When considering the solvent a polarizable continuum model (PCM), the theoretical spectra are very different from the experimental one. Particularly, the theoretical bands at c.a. 1740 cm^{-1}, that correspond to C = O stretching, overestimate in 80 cm^{-1} the experimental bands. Similar effects have been found in the DFT simulated spectra for several derivatives of DNA bases, with a PCM model for the solvent. [27] The inclusion of specific intermolecular interactions of the DNA bases derivatives with solvent molecules, improves the agreement between theoretical and experimental spectra. In our DFT simulations, inclusion of 2 or 3 D_2O molecules in the geometric optimization, originates simulated spectra closer to the experimental one. The results, including the main contributions to the bands, are summarized in Table S1

The keto-amino tautomer shows three strong bands at 1628, 1550 and 1523 cm^{-1} and a very weak band at 1499 cm^{-1}. In the keto-imino form, these bands with the same main vibrational contributions are shifted to 1632 (strong), 1594 (strong), 1575 (weak) and 1519 cm^{-1} (weak), respectively. The position and intensities of the bands corresponding to the keto-amino tautomer can explain the experimental G-5DP spectrum bands at 1662, 1579, 1565 and 1539 cm^{-1}, respectively, within a 3% of error in the wavenumbers and with similar relative intensities, as can be observed in Fig. S2. On the other hand, the set of bands corresponding to the keto-imino tautomer could explain the positions of the experimental bands, but not their relative intensities.

The results above suggest that the preponderant form of guanine in neutral solutions is the keto-amino form, in agreement with a previous work in the literature [28], where the assignments of the experimental Raman bands for neutral G-5DP in D_2O and H_2O solutions to vibratioknal modes of the keto-amino tautomer was made on the basis of ^{13}C, ^{15}N and ^{18}O substitution effects. The assignation of all the experimental bands in Fig. 2a given in [28], on the basis of the shifts upon isotopic substitutions, are coincident with the main vibrational contributions obtained from our DFT simulations, given in Table S1:The band at 1662 cm^{-1} corresponds to the stretching mode of the C6=O group, the band at 1579 is assigned to a pirimidin ring squeletal vibration with a large contribution of N3. The band at 1565 cm^{-1} was assigned to a pirimidin ring vibration with participation of C2. The remaining weak band at 1539 was assigned to a resonant vibration involving pyrimidine and imidazole rings.

Fig. 2b contains the FT-IR spectra of anionic guanine in solution at pD 11.6. It presents two overlapped strong bands at 1592 and 1570 cm^{-1} and a strong and very wide band, probably being the convolution of several bands, at 1463 cm^{-1}. The theoretical DFT spectra of canonical keto-amine tautomer of anionic guanine, incorporating two deuterated water molecules, included in Fig. S3, can explain most of the features of the absorption spectra of anionic guanine in solution: The experimental band at 1592 cm^{-1} can correspond to the C6=O stretching theoretical signal at 1619 cm^{-1}. The band at 1570 cm^{-1} matches to the theoretical bands 1565 (N3C4 stretching). The wide band observed at 1463 cm^{-1} can include the vibrations corresponding to the theoretical bands at 1482 cm^{-1} (C2N3+C1N2 stretching), 1452 (skeletal) and at 1434 cm^{-1} (C2N stretching). Table S2 summarizes the position and assignment. On the contrary, the theoretical spectrum for the keto-imine tautomer exhibit two main bands, one strong at 1615 cm^{-1} (C6=O stretching) and a very strong band at 1506 cm^{-1} (C2N stretching) that cannot explain the main features of the experimental spectrum of anionic guanine in solution. On the other hand, the presence of very weak experimental bands at 1649 cm^{-1}, 1538 and 1504 cm^{-1} suggests the minority presence of another tautomer of anionic guanine in solution.

3.3. *Spectroelectrochemical experiments of adsorbed guanine from solutions at pD 8*

ATR-SEIRA spectra of adsorbed guanine at −0.28 V and at 0.0 V, and potential averaged spectra are presented in Fig. 3. The complete set of spectra at different potentials is included in Fig. S4. The features of the ATR-SEIRA spectrum at −0.28 V in Fig. 3a are very similar to those of the transmission IR spectra of G-5DP (Fig. 2a), with one broad and intense band at 1669 cm^{-1}, and two close bands at 1601 and 1573 cm^{-1}. Therefore, it can be expected that the preponderant adsorbed guanine specie is the same as that in solution, the keto-amino tautomer. The surface selection rule in the ATR-SEIRA experiment, implicit in Eq. (1), requires that any active vibration mode have some component normal to the gold surface. Therefore, the presence of in plane vibrational bands in adsorbed state involves that guanine is adsorbed on gold with the molecular plane tilted, relative to the electrode surface. This is in good agreement with the work of Tao et al., demonstrating by AFM and STM that guanine ad-layers on gold are formed by polymeric aggregates in which the molecules are stacked with periodic distances of 3.3 ± 0.3 A, suggesting a highly tilted orientation of the molecular plane[13].

The ATR-SEIRA signal at 1668 cm^{-1} is quite wide, probably due to different C=O bands with different levels of solvation and/or the interaction with the electrode surface. When comparing to the spectrum of G-5DP in solution, it is observed that the adsorption of guanine also decreases the relative intensities of bands 1598 and 1573 cm^{-1} as

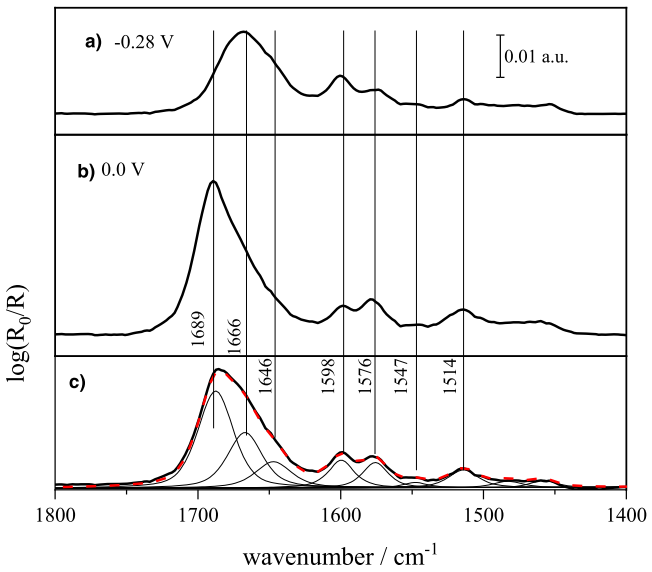

Fig. 3. a) ATR-SEIRA spectra in the 1800–1400 cm^{-1} region of guanine in D_2O solutions at pD 8 and -0.28 V vs SCE and b) at 0.0 V vs SCE. The potential values were constant during the spectral measurements. c) Potential averaged ATR-SEIRAS in the -0.3 to 0 V vs SCE range and its deconvolution into individual bands.

compared to the C=O group stretching. This effect becomes clearer as the potential increases. On considering the anisotropic character of the ATR-SEIRAS signals, it seems that guanine interacts with the gold electrode with the carbonyl group orientated close to the normal direction to the electrode surface. Moreover, the blue shift of the C=O stretching band in the adsorbed state suggests that the C=O group interacts with the electrode surface. This is confirmed by DFT geometrical optimization of keto-amino tautomer of guanine over a surface of 84 gold atoms 'frozen' into a (111) organization. The optimized geometry is showed in Scheme 2, with the molecular plane oriented normal to the electrode surface, with the carbonyl group directed towards the electrode in a hollow position. The molecular plane is slightly rotated (c.a. 6°) relative to the closest main direction of the gold crystal. The distances between the oxygen of carbonyl group and the closet gold atoms (Au_A, Au_B and Au_C) are 3.55, 3.55 and 3.28 Å, respectively Scheme 4.

At 0 V the ATR-SEIRAS spectrum shows the same number of bands that at −0.28 V. However, at this potential, the signal at 1668 cm^{-1} increases its intensity and shifts to 1689 cm^{-1}, probably due to the interaction with the electrode surface or changes in solvation. The frequencies of the bands around 1598 and 1573 cm^{-1} shift slightly with potential. However, their relative intensities change clearly, with the band at c.a. 1573 cm^{-1} becoming significantly higher than the band at c.

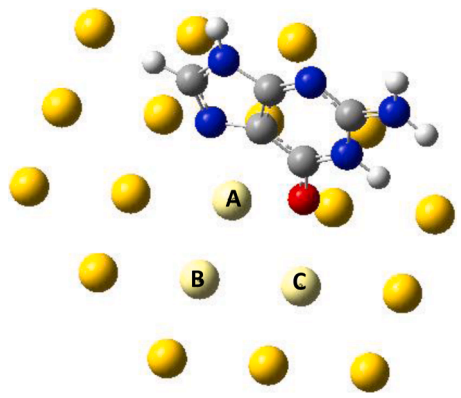

Scheme 4. Optimized geometries of G ND9 tautomer on gold atoms surface.

a 1600 cm^{-1} at 0 V. These intensity changes with potential may be due to reorientations of the molecular plane of guanine tautomer either by inclination or by rotation relative to the electrode surface.

Qualitatively, these changes could be better appreciated in the two-dimensional correlation spectra (2D COS). Fig. 4a and b show the synchronous and asynchronous 2D correlation spectra of adsorbed guanine from neutral D_2O solutions, the increasing potential being the external variable[29,30]. In both cases positive correlations are represented in red and the negative correlations are coloured blue.

Fig. 4a shows the synchronous spectra. The bands located off diagonal are cross-correlation bands, while the bands located at the diagonal are auto-correlation bands and are always positive. The positive sign of the cross-correlation bands indicates that they are changing in the same direction with the potential, and the negative sign indicates that they are changing in the opposite direction. Synchronous spectrum shows that the wide band observed in ATR-SEIRA spectra at 1680 cm^{-1}, which is related to C=O stretching of guanine, could involve at least two signals at c.a. 1646 and 1689 cm^{-1}. The synchronous spectrum is dominated by a strong blue square between 1646 and 1689 cm^{-1}. This indicates that these two bands are strongly correlated and change in the opposite direction. The cross-correlation bands of 1689 cm^{-1} with 1598 cm^{-1} and c.a. 1576 cm^{-1} are negative and positive, respectively, indicating that these changes are also correlated but their signs indicate that bands at 1598 cm^{-1} change with the potential in the opposite way that the C=O group of adsorbed guanine changes, while the band at 1576 cm^{-1} changes in the same manner. Moreover, the blue square between 1600 and 1580 cm^{-1} confirms that their intensities change in the opposite directions as qualitatively observed in Fig. 4a-b.

Fig. 4b plots the asynchronous spectrum. For a pair of bands denoted (ν_1, ν_2) with a positive sign of a cross-correlation band in the synchronous spectrum; positive sign of a cross-correlation band in the asynchronous spectra indicate that changes of the band at ν_1 take place before changes of ν_2. On the contrary, a negative sign indicates that ν_2 precedes ν_1. The asynchronous cross-correlation band (1689, 1646) is positive, while the synchronous correlation is negative. This means that changes with potential at 1689 cm^{-1} take place after changes at 1646 cm^{-1}, suggesting that two different physical phenomena are involved in the changes of the two bands with potential. The negative sign of the asynchronous correlations in the 1689–1598 bands and in 1690–1576, taking into account the synchronous correlations, suggest that the changes in the 1689 cm^{-1} band follow the changes of the 1598 cm^{-1} while changes of the 1689 cm^{-1} band precede changes of the 1576 cm^{-1}. Moreover, the absence of intense correlations in the asynchronous spectra at 1650–1600, 1650–1580, and 1600–1580 indicate that changes with the potential in the integrated intensities of those bands are synchronized. Considering that bands at 1650 and 1600 cm^{-1} decrease with the potential and band at 1580 cm^{-1} increases, the synchronized behavior could be explained if it is caused by a rotation of guanine molecular plane. On the other hand, the changes with the potential at 1690 cm^{-1} could be due to the stronger interaction of the carbonyl group with the electrode at higher potentials, as can be expected if guanine adsorbs with that group orientated towards the electrode, as it was suggested above.

To quantitatively analyze all the changes with the electrode potential in the ATR-SEIRA spectra of adsorbed guanine at pD 8, the deconvolution of the spectra into individual bands has been performed following the pattern showed in Fig. 3c for the potential-averaged spectrum, obtained from its second derivative (SD) and fourier self-deconvolution (FSD) (Fig. S5b and c, respectively). The assignment of these bands was based on our DFT calculation concerning solvated and adsorbed keto-amino tautomer and it is summarized in Table S1 in the SI file.

The most intense band in the ATR-SEIRAS spectra, around 1680 cm^{-1}, is deconvoluted into three bands at 1690, 1666 and 1646 cm^{-1}. Table S1 summarize the assignment of the experimental infrared signals, on the basis of the theoretical DFT spectra. Bands at 1689 cm^{-1} and 1666 cm^{-1} can be assigned to the carbonyl stretching band of adsorbed

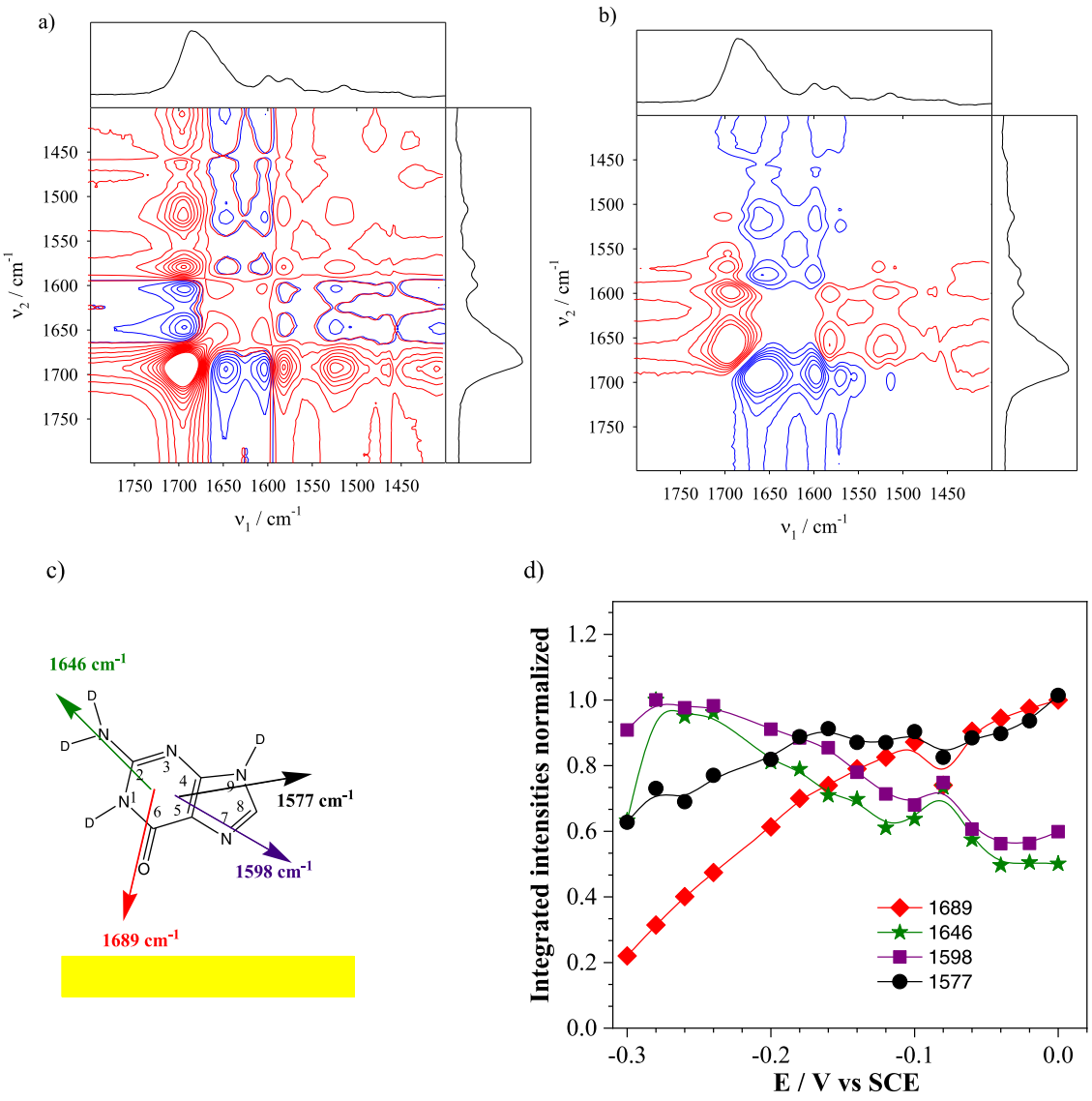

Fig. 4. a) Synchronous and b) asynchronous 2D COS results of the ATR-SEIRAS spectra for the 1800 and 1400 cm^{-1} regions of guanine in D_2O solutions at pD 8 using the electrode potential as external variable. Positive correlations are represented in red and negative correlations in blue. c) Structure of guanine indicating the approximate directions of the transition dipole moments of the signals indicated in the figure. d) Potential dependence of the integrated intensities (normalized to its maximum) of the main ATR-SEIRAS absorption bands of the spectra in Figure S4.

guanine and hydrated guanine, respectively. The main contribution of the experimental band at 1646 cm^{-1} is the C2N stretching. Bands at 1598 and 1576 cm^{-1} correspond to skeletal vibrations with different directions of the transition dipoles, as can be observed in Fig. 4c).

Fig. 4d contains the integrated intensities of the main absorption bands of adsorbed guanine normalized to their maximum values (obtained in the deconvolution of the ATR-SEIRA spectra) represented as a function of the applied potential. The intensity of the band at 1666 cm^{-1} remains almost constant (not plotted), indicating the presence of some solvated guanine not strongly adsorbed on the electrode. The band at 1689 cm^{-1} continuously increases its intensity with the potential in the range explored, indicating the increasing number of guanine molecules with a stronger interaction of the carbonyl group with the electrode surface. The parallel decrease with the potential of the integrated intensities at 1646 and 1598 cm^{-1} and the increases of the intensity at 1576 cm^{-1} can be explained by a small rotation of the molecular plane of guanine with the potential, so the transition dipoles of the vibrations at 1646 and 1598 cm^{-1} (almost along the same direction within the molecular plane) become more parallel to the electrode surface, while the transition dipole of the vibration at 1576 becomes less parallel as the potential increases. According to the approximate directions of the vibrational dipoles represented in Fig. 4c), the described rotation would be counterclockwise. This rotation movement would also contribute to increase the integrated intensity of the C=O stretching band at 1689 cm^{-1}.

3.4. Spectroelectrochemical experiments of adsorbed guanine at pD 11.6

Fig. 5a and b show ATR-SEIRA spectra of guanine adsorbed on gold nanofilm electrodes in the 1800–1400 cm^{-1} region at pD 11.6 at two different potential values. Both spectra are very different from the transmission spectra of anionic guanine at pD 11.6 (Fig. 2b), particularly at −0.1 V, and include a higher number of spectral bands, as can be observed in the deconvolution of the potential averaged ATR-SEIRA spectrum in Fig. 5c.

At −0.58 V the ATR-SEIRAS spectra includes a wide carbonyl signal at c.a. 1650 cm^{-1}, that must correspond to the weak signal obtained at 1649 cm^{-1} for guanine in solution. As the potential increases to −0.1 V, the relative intensity of the carbonyl signal increases, and it shifts to a higher wavenumber, compared to the spectrum in solution (Fig. 2b). The

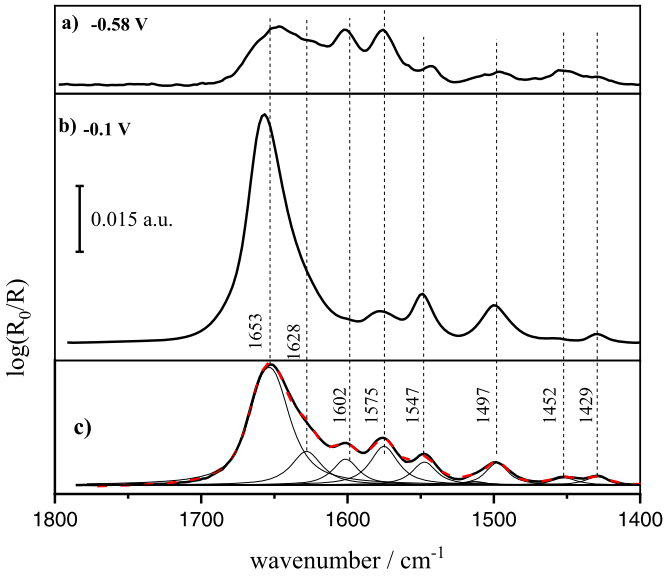

Fig. 5. a)ATR-SEIRA spectra in the 1800–1400 cm^{-1} region of anionic guanine in D_2O solutions at pD 11.6 at -0.58 V and b) -0.1 V. c) Potential averaged ATR-SEIRAS in the -0.8 to -0.1 V vs SCE range and its deconvolution into individual bands.

observed shift (c.a. 60 cm^{-1}) in the position of the carbonyl-stretching band upon adsorption cannot be explained as an exclusive consequence of the loss of hydration and the interaction with the electrode, although these facts could also contribute. On the other hand, the appearance of new spectral bands, corresponding to skeletal vibrations, suggest the presence of a new tautomeric form in the adsorbed state. The comparison of the spectra at the two potentials, shown in Fig 5a and b, indicates that this new form is favored at higher potentials. This is also supported by the 2D-COS synchronous spectra, with the potential as external variable, shown in Fig. 6a. The cross-correlations show two sets of bands, changing in the opposite way with the potential: bands at c.a. 1650, 1550 and 1500 cm^{-1} change in the same direction with the potential, and bands at c.a. 1600, 1570 and 1450 cm^{-1} change in the opposite direction. On the contrary, the asynchronous 2D-COS (not shown) does not exhibit significant correlations, either positive or negative, indicating that all the spectral changes with the potential are synchronized and that could be caused by the same physical phenomena.

Fig. 5c includes the deconvolution of the potential averaged ATR-SEIRA spectrum of guanine adsorbed from solutions at pD 11.6, using the pattern obtained from its second derivative (SD) and Fourier self-deconvolution (FSD), with the exact position of the individual bands indicated. The bands at 1602 and 1575 cm^{-1} of adsorbed anionic guanine, which initially increase with the potential up to c.a.−0.55 V and decrease at higher potentials, can correspond to the bands at 1592 and 1570 cm^{-1} of anionic guanine in solution (Fig. 2b), in principle assigned to the keto-amino tautomeric form. This behavior could be explained if at low potentials, the increasing potential increases also the tilt angle and/or the surface concentration of the keto-amino form of the anionic guanine adsorbed, up to −0.55 V vs SCE, at which the keto-imino tautomer becomes more relevant in adsorbed state and gradually sweep the keto-amino from the surface, as the potential increases. This

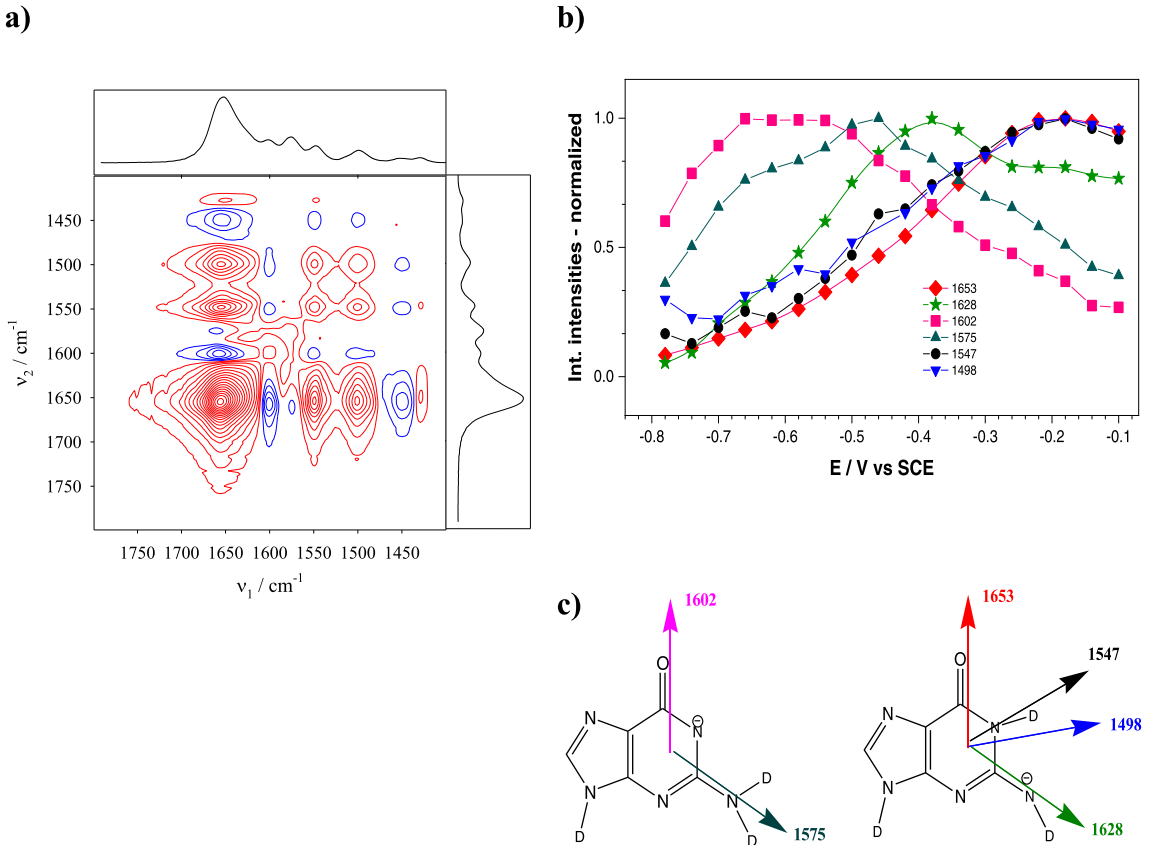

Fig. 6. a) Synchronous 2D COS results of the ATR-SEIRAS spectra for the 1800 and 1400 cm^{-1} regions of guanine in D_2O solutions at pD 11, with the increasing potential being the external variable. Positive correlations are represented in red, and negative correlations in blue.b) Potential dependence of the integrated intensities of the main ATR-SEIRAS absorption bands obtained from the deconvolution with the pattern obtained in a). c) Structure of keto-amino and keto-imino forms of anionic guanine indicating the approximate transition dipole moments directions of the signals indicated in the figure. b)

potential onset is almost coincident with one of the capacitance peaks in Fig. S1. The bands at 1653, 1628, 1547 and 1498 cm^{-1}, which increase with the potential up to c.a. −0.2 V vs SCE, must correspond to a different tautomeric form of anionic guanine adsorbed. The intense band at 1653 cm^{-1} can be assigned to a carbonyl stretching vibration, suggesting that the new tautomeric form favoured at high potentials could be the keto-imino tautomer of anionic guanine. DFT simulation of this tautomer adsorbed on gold (111) indicates that it adsorbs with the molecular plane normal to the electrode and the carbonyl group and N7 orientated towards the surface. The corresponding simulated IR spectrum, in Fig. S3, contains bands at 1673, 1639, 1545 and 1470 cm^{-1} that match with the experimental bands at 1663, 1628, 1547 and 1498 cm^{-1} of the ATR-SEIRA spectra, supporting that the keto-imino tautomer is the form of anionic guanine favoured in adsorbed state at high potentials. The assignment of these bands is included in Table S2. It must be noted here that spectrum of anionic guanine in solution, in Fig. 2b, also includes weak or very weak bands at 1649, 1528 and 1504 cm^{-1} that could also be explained as caused by a minor presence of the keto-imino tautomer of anionic guanine in solution. The simulated band at 1639 cm^{-1}, could explain the experimental ATR-SEIRA band at 1628 cm^{-1}, corresponds to the C2N stretching vibration of the keto-imino form.

The transition dipoles of these individual bands, according to their assignation in Table S2, show very different directions within the molecular plane of anionic guanine, as can be observed d in Fig. 6c. According to Eq. (1), any change in the rotation of the molecular plane with the potential would involve changes in the relative intensities of the bands corresponding to in-plane vibrations with different directions of the transition dipole. However, changes in the tilt angle of the molecular plane, defined as the angle between the normal direction to the plane and the normal direction to the electrode, would affect with the same factor every in-plane vibration. Then, the parallel increase and decrease with the potential of the two signal groups can only be caused by changes in the surface concentration or in the tilt angle of the molecular plane of the keto-amino form of adsorbed anionic guanine decreases with the potential, at potentials higher than −0.55 V vs SCE and the surface concentration or tilt angle of the adsorbed keto-imino form increases with the potential up to c.a. −0.2 V vs SCE.

4. Conclusions

The comparison of FT-IR spectra in solution for G 5DP guanine at pD 8 and pD 11 with DFT vibrational spectra simulations indicates the preponderance in solution of the solvated keto-amino tautomer form for neutral and anionic guanine, respectively.

The ATR-SEIRA spectra of adsorbed guanine from solutions at pD 8 indicate that the species adsorbed from neutral media is the same as the neutral guanine form existing in solution, the keto-amino tautomer. The shift observed in the position of the C=O stretching band upon adsorption indicates the loss of hydration and the direct interaction of the C=O group with the electrode. Moreover, the presence of in-plane vibrational bands indicates a highly tilted orientation of the molecular plane of adsorbed guanine. DFT calculated spectra of adsorbed keto-amino tautomer on gold clusters support these conclusions. The evolution of the integrated intensity of the spectral bands with the increasing potential can be explained by a rotation of the molecular plane of adsorbed keto-amino tautomer, which makes the direction of the C=O group closer to the normal direction to the electrode.

At pH 11.6, the differences in the spectrum in solution respect to the DFT spectrum of the keto-amino form of anionic guanine cannot be explained by solvation effects, especially at high potentials, but by some contribution of the keto-imino tautomer. The analysis of the evolution of the spectra with potential reveals two different potential regions of adsorption. At potentials below c.a. −0.55 V vs SCE the favored form adsorbed is the keto-amino, as at pD 8, but at higher potential values the keto imino form is the favored one.

CRediT authorship contribution statement

Julia Alvarez-Malmagro: Investigation, Formal analysis, Writing – original draft. **Manuela Rueda:** Conceptualization, Supervision, Funding acquisition. **Francisco Prieto-Dapena:** Conceptualization, Supervision, Formal analysis, Writing – review & editing, Funding acquisition.

Declaration of Competing Interest

I hereby manifest that I have not any conflict of interest with the submission and publication of the manuscript. This applies for the past, the present and the foreseeable future.

Data availability

Data will be made available on request.

Acknowledgments

This research was funded by Junta de Andalucía (Spain) FQM-202 and the University of Sevilla grant number 2021/00001268. The authors want to thank Centro de Servicios de Informatica y Redes de Comunicaciones (CSIRC) of University of Granada for the computing time. and the general services (CITIUS) of Seville University for the technical support provided.

Supplementary materials

Supplementary material associated with this article can be found, in the online version, at doi:10.1016/j.electacta.2023.142465.

References

[1] J. Liu, Adsorption of DNA onto gold nanoparticles and graphene oxide: surface science and applications, Phys. Chem. Chem. Phys. 14 (2012) 10485–10496, https://doi.org/10.1039/c2cp41186e.
[2] Y.H. Jang, W.A. Goddard, K.T. Noyes, L.C. Sowers, S. Hwang, D.S. Chung, pKa values of guanine in water: density functional theory calculations combined with Poisson-Boltzmann continuum-solvation model, J. Phys. Chem. B. 107 (2003) 344–357, https://doi.org/10.1021/jp020774x.
[3] P.S. Liss, P.G. Slater, The double helix: a personal view, Nature 248 (1974) 766–769.
[4] M.D. Topal, J.R. Fresco, Complementary base pairing and the origin of substitution mutations, Nature 263 (1976) 285–289, https://doi.org/10.1038/263285a0.
[5] L.C. Sowers, B.R. Shaw, M.L. Veigl, W.David Sedwick, DNA base modification: ionized base pairs and mutagenesis, Mutat. Res. 177 (1987) 201–218, https://doi.org/10.1016/0027-5107(87)90003-0.
[6] R.P. Lopes, M.P.M. Marques, R. Valero, J. Tomkinson, L.A.E.B. de Carvalho, Guanine: a combined study using vibrational spectroscopy and theoretical methods, Spectrosc. An Int. J. 27 (2012) 273–292, https://doi.org/10.1155/2012/168286.
[7] A.K. Chandra, M.T. Nguyen, T. Uchimaru, T. Zeegers-Huyskens, Protonation and deprotonation enthalpies of guanine and adenine and implications for the structure and energy of their complexes with water: comparison with uracil, and Cytosine, J. Phys. Chem. A. 103 (1999) 8853–8860. doi:10.1021/jp990647+.
[8] V.H. Harris, C.L. Smith, W.Jonathan Cummins, A.L. Hamilton, H. Adams, M. Dickman, D.P. Hornby, D.M. Williams, The effect of tautomeric constant on the specificity of nucleotide incorporation during DNA replication: support for the rare tautomer hypothesis of substitution mutagenesis, J. Mol. Biol. 326 (2003) 1389–1401, https://doi.org/10.1016/s0022-2836(03)00051-2.
[9] D.Y. Wu, L. Ugozzoli, B.K. Pal, R.B. Wallace, Allele-specific enzymatic amplification of β-globin genomic DNA for diagnosis of sickle cell anemia, Proc. Natl. Acad. Sci. U. S. A. 86 (1989) 2757–2760, https://doi.org/10.1073/pnas.86.8.2757.
[10] Y. Yang, D.S. Geldmacher, K. Herrup, DNA replication precedes neuronal cell death in Alzheimer's disease, J. Neurosci. 21 (2001) 2661–2668, https://doi.org/10.1523/jneurosci.21-08-02661.2001.
[11] Z. Shi, F. International, I. Final, monolayer guanine and adenine on graphite in NaCl solution: a comparative STM and AFM study, J. Phys. Chem. 98 (1994) 1464–1471.
[12] R. Srinivasan, J.C. Murphy, R. Fainchtein, N. Pattabiraman, Electrochemical STM of condensed guanine on graphite, J. Electroanal. Chem. 312 (1991) 293–300, https://doi.org/10.1016/0022-0728(91)85161-H.

[13] N.J. Tao, J.A. De Rose, S.M. Lindsay, Self-assembly of molecular superstructures studied by in situ scanning tunneling microscopy: DNA bases on Au(111), J. Phys. Chem. 97 (1993) 910–919, https://doi.org/10.1021/j100106a017.
[14] K. Takamura, A. Mori, F. Watanabe, Structural effects of nucleic acid bases, nucleosides and nucleotides on their adsorption at a gold electrode studied by specular reflectivity measurement, J. Electroanal. Chem. Interfac. Electrochem. 128 (1981) 125–136, https://doi.org/10.1016/S0022-0728(81)80193-3.
[15] E.E. Ferapontova, Electrochemistry of guanine and 8-oxoguanine at gold electrodes, Electrochim. Acta. 49 (2004) 1751–1759, https://doi.org/10.1016/j.electacta.2003.12.006.
[16] E.T.O. Measure, A. In, The use of glass electrode to measure acidities in deuterium oxide, J. Phys. Chem. 267 (1952) 188–190.
[17] J. Clavilier, R. Faure, G. Guinet, R. Durand, Preparation of monocrystalline Pt microelectrodes and electrochemical study of the plane surfaces cut in the direction of the {111} and {110} planes, J. Electroanal. Chem. Interfac. Electrochem. 107 (1980) 205–209, https://doi.org/10.1016/S0022-0728(79)80022-4.
[18] M. Osawa, K.-.I. Ataka, K. Yoshii, Y. Nishikawa, Surface-enhanced infrared spectroscopy: the origin of the absorption enhancement and band selection rule in the infrared spectra of molecules adsorbed on fine metal particles, Appl. Spectrosc. 47 (1993) 1497–1502, https://doi.org/10.1366/0003702934067478.
[19] J. Alvarez-Malmagro, Z. Su, J.J. Leitch, F. Prieto, M. Rueda, J. Lipkowski, Electric-field-driven molecular recognition reactions of guanine with 1,2-dipalmitoyl- sn-glycero-3-cytidine monolayers deposited on gold electrodes, Langmuir 35 (2019) 9297–9307, https://doi.org/10.1021/acs.langmuir.9b01238.
[20] M.J. Frisch, G.W. Trucks, H.B. Schlegel, G.E. Scuseria, M.A. Robb, J.R. Cheeseman, G. Scalmani, V. Barone, B. Mennucci, G.A. Petersson, H. Nakatsuji, M. Caricato, X. Li, H.P. Hratchian, A.F. Izmaylov, J. Bloino, G. Zheng, D.J. Sonnenb, Gaussian, 09, Gaussian, Inc, Wallingford CT, 2016.
[21] P.C. Hariharan, J.A. Pople, The influence of polarization functions on molecular orbital hydrogenation energies, Theor. Chim. Acta. 28 (1973) 213–222, https://doi.org/10.1007/BF00533485.
[22] T. Clark, C. Jayaraman, G.W. Spitznagel, P. Von Ragué Schleyer, Efficient diffuse function-augmented basis sets for anion calculations. III. The 3-21+ G basis set for first-row elements Li–F, J. Comput. Chem. 4 (1983) 294–301.
[23] Elke Goos, György Lendvay, Calculation of molecular thermochemical data and their availability in databases. Cleaner Combustion, Springer, London, 2013, pp. 515–547, n.d.
[24] I.M. Alecu, J. Zheng, Y. Zhao, D.G. Truhlar, Computational thermochemistry: scale factor databases and scale factors for vibrational frequencies obtained from electronic model chemistries, J. Chem. Theory Comput. 6 (2010) 2872–2887, https://doi.org/10.1021/ct100326h.
[25] J. Álvarez-Malmagro, F. Prieto, M. Rueda, A. Rodes, In situ Fourier transform infrared reflection absorption spectroscopy study of adenine adsorption on gold electrodes in basic media, Electrochim. Acta. 140 (2014) 476–481, https://doi.org/10.1016/j.electacta.2014.03.074.
[26] H. DeVoe, S.P. Wasik, Aqueous solubilities and enthalpies of solution of adenine and guanine, J. Solut. Chem. 13 (1984) 51–60, https://doi.org/10.1007/BF00648591.
[27] M. Shanmugasundaram, M. Puranik, Computational prediction of vibrational spectra of normal and modified DNA nucleobases, J. Raman Spectrosc. 40 (2009) 1726–1748, https://doi.org/10.1002/jrs.2533.
[28] A. Toyama, N. Hanada, J. Ono, E. Yoshimitsu, H. Takeuchi, Assignments of guanosine UV resonance Raman bands on the basis of13C, 15 N and18O substitution effects, J. Raman Spectrosc. 30 (1999) 623–630, https://doi.org/10.1002/(SICI)1097-4555(199908)30:8<623::AID-JRS407>3.0.CO;2-9.
[29] I. Noda, Two-dimensional codistribution spectroscopy to determine the sequential order of distributed presence of species, J. Mol. Struct. 1069 (2014) 50–59, https://doi.org/10.1016/j.molstruc.2014.01.024.
[30] I. Noda, A.E. Dowrey, C. Marcott, G.M. Story, Generalized two-dimensional correlation spectroscopy, Appl. Spectrosc. 54 (2000) 236A–248A, https://doi.org/10.1366/0003702001950454.